APPENDIX – I

Revised Flooding Rate Bounds

Note: This appendix was originally added in its entirety in Revision 5 of BAW-10166 for the purpose of extending the range of applicability to lower flooding rates.

I.1 Introduction

This appendix justifies a revision to the lower boundary on the BEACH code (Reference I-1) reflood flooding rate range of applicability. BEACH is currently restricted to flooding rates equal to or above 0.5 in/s. The possibility of predicting flooding rates of less than 0.5 in/s was identified recently. The extension of the range of applicability from 0.5 in/s to 0.3 in/s is justified through comparisons with experiments, including some previously used in the approved BEACH topical report (Reference I-1).

The NRC safety evaluation report (SER) for Revision 2 of the BEACH topical report (Reference I-1, pages 5-228 and 5-229) restricts the applicability of the code to a specified flooding rate range. The SER states:

"In using the revised grid and rupture models with the recommended empirical values of the droplet breakup number, n, of 2.7 and the volume length constant, C_1, of 1.22 meters, the user should ensure that the models are applied to the plant conditions within the applicable ranges for which the empirical constants were assessed, or must supply additional justification to justify the use. The applicable ranges are as follows:

Peak power:	0.4 – 1.0 kW/ft
Containment backpressure:	15 – 73 psia
Cladding temperature:	950 – 1640 ^{o}F
Core inlet subcooling:	0.0 – 180 ^{o}F
Flooding rate:	**0.5 – 10.0 in/s**
Grid flow blockage:	0.0 – 0.55
Rupture flow blockage:	0.0 – 0.60"

The flooding rate range listed in the SER was derived through consideration of the experimental benchmarks provided in support of BEACH. The benchmarks were largely forced flooding experiments at constant flooding rates and the limits are expressed in terms of instantaneous flooding rates. The lowest flooding rate previously benchmarked was 0.6 in/s and the lower limit of 0.5 in/s represents a small, NRC approved, extrapolation from the range of the benchmark cases.

The revised lower limit on the flooding rate justified in this appendix is 0.3 in/s. Four sets of benchmarks are presented in this appendix. The benchmarks demonstrate the acceptability of BEACH predictions down to an instantaneous flooding rate of 0.3 in/s. Section I.2 provides benchmarks to low flooding rate FLECHT-SEASET tests. These are complemented in Section I.3 with benchmarks to the FLECHT series of tests. Both test series approximate the conditions expected in a reactor—variable flooding rates evolving to a slowly decreasing flooding rate. To demonstrate the realistic variable flooding rate case, two gravity reflood tests that result in a low, 0.4 in/s, flooding rate are benchmarked in Section I.4. BEACH-predicted and experimental differential temperature rises versus the ratio of flooding rate to peak power are compared in Section I.6. The results demonstrate the acceptability of BEACH predictions down to flooding rates of 0.3 in/s.

I.2 FLECHT-SEASET Tests

Five FLECHT-SEASET tests (References I-2 through I-4) were selected to provide additional BEACH benchmarks. Two of the tests (Tests 35807 and 35912) provide comparisons at lower flooding rates, ~0.4 in/s. The other three tests (Tests 31701, 31203, and 34006) demonstrate the general performance of the BEACH code at higher flooding rates and provide input for the differential temperature rise discussion in Section I.6.

The five tests are forced reflood tests, conducted in the 161-rod bundle FLECHT-SEASET test facility (Reference I-3). The test conditions are given in Table I-1. The BEACH input model is the same as that used in the previous FLECHT-SEASET benchmarks reported in Reference I-1, Appendix G. The fuel pin array upon which the unit cell is based is shown in Figure D-1 (Reference I-1). The noding and axial power distribution are shown in Figure D-3 (Reference I-1). In Appendix G, lower and upper unheated pin regions were added to the model shown in Figure D-2 to mimic the B&W plant nodalization technique. In Appendix G (Section G-2), it is concluded that the calculated PCT results were unchanged by the addition of the unheated nodes.

Therefore, although there are no unheated nodes in the RSG plant model, for continuity the model used in Appendix G is also used in these benchmarks.

Significant bundle distortion occurred in the center of the test bundle between the 60- and 90-inch elevations for tests conducted after Test 34610. The test summary on page 1-2 of Reference I-3 states: “beyond Test 34610, the distortion cannot be ignored; data above 1.52 m (60.0 inch) elevation should not be used for heat transfer development.” Since Tests 35807 and 35912 were conducted after Test 34610, the data above 5.0 ft cannot be used for code evaluation purposes.

For Tests 35807 and 35912, the power in the center power zone was lower than specified by approximately 10 and 12 percent, respectively. Figure G-9 of the test report (Reference I-3) shows the heater rod power groups. It can be seen that the bundle is connected to three power zones: group-1, group-2, and group-3. Since the major portion of the central rods is connected to the center power zone (group-1), the power decay in the input model is reduced by 10 percent for Test 35807 and 12 percent for Test 35912 from that of the Test 31504 input model.

The cladding temperatures calculated by the BEACH code agree well with the measured cladding temperatures for Tests 31701, 31203, and 34006. For Tests 35807 and 35912, BEACH agrees with the data for elevations below the bundle distortion. Figures I-1 through I-5 show the measured and predicted peak clad temperatures (PCT) as a function of elevation for the five tests. From Figures I-1 and I-2, it can be seen that data for the group-1 rods above the 6-ft location are higher than that for group-2 and group-3, even though the group-1 rods have a lower power than the group-2 and group-3 rods. This may be caused by the significant bundle distortion above the 5-ft location in Tests 35807 and 35912. This conclusion is supported by the observation that the results for the other three tests show that the temperatures for all three groups of rods are about the same.

Although data from pin location above 5 feet can be questioned, the BEACH predictions of quench front advancement are in reasonable agreement with the measurements throughout the transient. Figures I-6 and I-7 show the measured and predicted quench front variation with time for Tests 35807 and 35912. Quench front advancement is discussed further in Section I.5.

These comparisons of calculated and measured results demonstrate the acceptability of BEACH predictions with instantaneous flooding rates as low as 0.4 in/s.

I.3 FLECHT Forced Reflood Tests

To benchmark the FLECHT test series, two low flooding tests were selected. Tests 8037 (Reference I-5) and 0791 (Reference I-6) are forced reflood tests, conducted in the 10x10 array bundle FLECHT test facility (Reference I-8). The test conditions are given in Table I-1. The test bundle, shown in Figure 2.2 of Reference I-8, consists of 91 full-length (12 ft heated length) solid electrical fuel rod simulators. The 0.422-inch diameter rods were arranged in a 0.563-inch square pitch typical of a 15x15 PWR fuel configuration (see Table 2-2 in Reference I-8). The rods were held together using eight FLECHT-type simple egg-crate (see page 2-14 in Reference I-8) support grids. The rods are internally heated with a 1.66 peak-to-average chopped cosine axial power shape as shown in Reference I-5, Figure A-1. The details of the fuel rod design are shown in Reference I-5, Figures B-1 and C-1. The test heater rods operate at three radial power levels—1.1, 1.0, and 0.95 compared to the average power rod—to obtain radial power variation (see Reference I-8, Figure 3-3). The BEACH benchmarks provided here simulate only the average power rod with a radial peaking of 1.0.

The BEACH code conservatively predicted the PCTs for both Test 8037 and Test 0791. Figures I-8 and I-9 show the measured and predicted PCTs as a function of elevation for Test 8037 and Test 0791, respectively. Figures I-10 and I-11 show the measured and predicted quench front variation with time. BEACH underpredicts quench front advancement for Test 0791 but overpredicts the advancement for Test 8037. Figures I-12 and I-13 show the measured and predicted cladding temperature variations with time near the 6.0-ft location for both tests.

The comparisons of BEACH calculated results and measured results for the above tests provide benchmark support for the BEACH code with instantaneous flooding rates as low as 0.4 in/s.

I.4 FLECHT Gravity Reflood Tests

To demonstrate that the BEACH code remains conservative for the realistic variable flooding rate situation, two gravity reflood tests from the FLECHT-SET PHASE B series were benchmarked. Actual plant behavior during large break LOCA does not involve long slow reflooding at low flooding rates. Rather the core is initially refilled at a high rate that decreases to a low flooding rate. Therefore, as the transient approaches a low reflood rate, the quench front behaves differently than it does for a constant, low flooding rate experiment.

The FLECHT-SET PHASE B facility was designed to simulate the primary coolant system of a PWR during the reflood phase of LOCA. The facility consists of a 10x10-rod bundle with a 12-foot heated length, simulated intact and broken loops with active steam generators, a downcomer, a lower plenum, and an upper plenum. The rod bundle used in these tests is the same as that used in the FLECHT low flooding rate cosine tests described in Section I.3. The facility design is described in detail in Reference I-8. Twenty tests were conducted in the Phase-B test series. For each test, coolant injection began when the system reached the specified initial test condition. When the water level reached the bottom of the heated length, the power supplied to the rods was controlled to follow the decay power as specified by the 1971 ANS 5.1 standard plus 20 percent. For each test, the containment pressure, upper plenum-to-containment differential pressure, lower plenum fluid temperature, and rod surface temperatures at various locations were measured. The mass flow into the test section and the flooding rate were estimated from a mass balance of the downcomer, the overflow tanks, and the containment tank. The tests, test procedure, and flooding rate calculations are discussed in the test data report (Reference I-7) and in the evaluation report (Reference I-10).

The flooding rate for Tests 3215B and 3316B falls to between 0.3 and 0.5 in/s after about 20 seconds. Therefore, these two tests were selected to benchmark the BEACH code. Test initial conditions are given in Table I-1.

The BEACH input model is same as that used in the FLECHT forced reflood tests benchmarks described in Section I.3. The upper plenum pressure and flooding rate inputs to the Test 3215B simulation are shown in Figures I-14 and I-15, respectively. The upper plenum pressure is calculated from the measured containment pressure and the upper plenum-to-containment ΔP. In the tests, the lower plenum fluid temperature remained constant at 149^{o}F. In the BEACH model, the fluid temperature is set to 149^{o}F in the time dependent volume that represents the lower plenum.

The upper plenum pressure and flooding rate inputs to the Test 3316B simulation are shown in Figures I-16 and I-17, respectively. Even though the containment pressure from Table 4-1 in Reference I-7 is 19 psia, the containment pressure plot in the figure on page 3316-18 of Reference I-7 shows that the pressure is ~55 psig at the beginning of the transient. At around 300 seconds, the pressure drops to about 5 psig. Such a pressure decrease should have created a significant core mixture swell with an impact on upper region cladding temperatures. However, the measured results are mixed. The cladding temperatures for Test 3316B are somewhat lower than those for Test 3215B but at least one data set (TC 4 in Figure I-23) remains elevated until about 400 seconds. The actual pressure course for this test, therefore, is questionable. Despite this concern, the simulation used the published measurements of pressure and differential pressure to specify the upper plenum pressure with the resultant consequences to the predictions. In the test, the lower plenum fluid temperature varied linearly from 204^{o}F at the beginning of the transient to 211^{o}F at 560 seconds. In the BEACH model, these values are input in the time dependent volume that represents the lower plenum.

The BEACH-predicted PCTs approximate the data below the 4-foot elevation. They are substantially conservative for positions above 4 feet for Tests 3215B and 3316B. Figures I-18 and I-19 show the measured and calculated PCTs as a function of elevation for Test 3215B and Test 3316B, respectively.

Figures I-20 and I-21 show the measured and predicted quench front variations with time. BEACH correctly predicted the bottom-up quench front advancements for both tests. The drop in the predicted quench front at approximately 300 seconds is a result of flashing caused by the rapid pressure decrease from 55 to 5 psig. This effect is not fully recognized in the data but may be indicated by the small drop in measured quench front at 300 seconds. Regardless, the prediction is reasonable or conservative for bottom up quenching. Top-down quenching is also present in both tests; this phenomenon is not modeled in BEACH. The existence of top-down quenching suggests liquid flows down through some of the sub-channels. This down flow is apparently responsible for the lower PCTs in the upper bundle regions. Figures I-22 and I-23 show the measured and predicted cladding temperature variations with time near the 6.0-ft location for both tests.

The comparison of the calculated and the measured results for the above tests provides further evidence of proper code performance for instantaneous flooding rates as low as 0.4 in/s.

I.5 Evaluation of Quench Front Advancement

The BEACH predicted quench front advancement behavior presented in the previous sections is generally conservative. BEACH predicts reasonably good quench front advancement for all benchmarks below the 6-foot quench front position. As the quench front advances to higher elevations, BEACH predicts a faster quench front advancement than the data for Test 35807, Test 35912, and Test 8037. However, the bundle distortion that occurred in Test 35807 and Test 35912 makes the measured results above 5 feet for two of these three tests questionable. For Test 0791, BEACH predicts a slower quench front advancement than the data. Setting aside top-down quenching, BEACH correctly predicts quench front advancement for the gravity reflood tests (Test 3215B and Test 3316B). These tests have the realistic variable flooding rates. Overall, BEACH quench front advancement provides an adequate and sufficient quench front simulation.

I.6 Differential Temperature Rise Benchmarks

The following discussion demonstrates the adequacy of using BEACH to simulate core heat transfer for flooding rates as low as 0.3 in/s. This justification relies on the behavior of ΔT_{RISE}, the differential temperature rise, which is the difference between the initial cladding temperature and the PCT as measured in the experiment of interest. ΔT_{RISE} increases with decreasing V_{in}/Q or a lower initial cladding temperature. V_{in} is the core flooding rate and Q is the assembly power.

ΔT_{RISE} is a weak function of pressure or inlet subcooling. These dependencies were evaluated in Section 3 of Reference I-2.

Table I-1 provides the initial conditions for the tests used to benchmark BEACH. Table I-2 tabulates ΔT_{RISE} and V_{in}/Q for the FLECHT SEASET tests and the corresponding results from BEACH. In Addition, four additional cases were evaluated using BEACH for successively lower flooding rates of 0.72, 0.60, 0.45, and 0.36 in/s, which were based on the conditions of Test 31504. These results, identified as “ftesta_1 through ftesta_4” in Table I-2, show ΔT_{RISE} increasing as V_{in}/Q decreases, as predicted.

Table I-3 provides selected results from the FLECHT tests. For the two tests with the lowest flooding rate (0.4 in/s) ΔT_{RISE} is also provided from BEACH analyses.

In most cases BEACH conservatively predicts ΔT_{RISE}. The exceptions are Test 31701, which is a high flooding rate test with a very small value of ΔT_{RISE}, and Tests 35912 and 0791, for each of which the experimental and predicted ΔT_{RISE} is nearly identical. The increase in ΔT_{RISE} with smaller values of V_{in}/Q is consistent for all benchmark cases, except for the apparent aberration of Test 31504 in the first grouping in Table I-2. This is actually caused by the large ΔT_{RISE} calculated for Test 34006. Test 34006 is the only low power case in this grouping. The lower power leads to a calculated ΔT_{RISE} excessive in comparison with the rest of the group. With Test 34006 removed, the predicted trend of ΔT_{RISE} is smooth and monotonic.

A summary of the results is shown in Figure I-24, which provides a plot of ΔT_{RISE} for a wide range of V_{in}/Q for the available data and for the BEACH results. Although parameter variations in both the predictions and the experiments create some dispersion, proper trending is evident in both the data and the BEACH predictions.

The consistency of the BEACH-calculated trend of ΔT_{RISE} versus V_{in}/Q and the conservatism of the results relative to test data justify the use of a 0.3 in/s lower bound on the instantaneous flooding rate range.

I.7 Conclusions

The SER for Revision 2 of the BEACH topical report (Reference I-1) restricts the applicability of the code to flooding rates at or above 0.5 in/s. Two FLECHT-SEASET benchmark cases (Test 35807 and Test 35912), two FLECHT benchmark cases (Test 8037 and Test 0791), two gravity-feed benchmark cases (Test 3215B and Test 3316B), and a trend analysis for differential temperature rise are provided. These benchmarks demonstrate that BEACH predictions are valid and conservative down to 0.3 in/s instantaneous flooding rates. It is concluded that BEACH conservatively predicts PCT for flooding rates of 0.3 in/s and above to the previously applied upper limit.

I.8 References

I-1. BEACH Code Topical Report, BAW-10166P-A, Revision 4, February 1996.

I-2. N. Lee, S. Wong, H.C. Yeh, and L.E. Hochreiter, PWR FLECHT-SEASET Unblocked Bundle, Forced and Gravity Reflood Task Data Evaluation and Analysis Report, NUREG-CR-2256, November 1981.

I-3. M. J. Loftus, et al., PWR FLECHT-SEASET Unblocked Bundle, Forced and Gravity Reflood Task Data Report, Volume 1, NUREG/CR-1532, June 1980.

I-4. M. J. Loftus, et al., PWR FLECHT-SEASET Unblocked Bundle, Forced and Gravity Reflood Task Data Report, Volume 2, NUREG/CR-1532, September 1981.

I-5. E. R. Rosal, et al., FLECHT Low Flooding Rate Cosine Test Series Data Report, WCAP-8651, December 1995.

I-6. F. F. Cadek, et al., PWR FLECHT Final Report Supplement, WCAP-7931, October 1972.

I-7. J. P. Waring, et al., PWR FLECHT-SET Phase B1 Data Report, WCAP-8431, December 1974.

I-8. W. F. Cleary, et al., FLECHT-SET Phase B System Design Description, WCAP-8410.

I-9. FLECHT Low Flooding Rate Skewed Test Series Data Report, WCAP-9108, May 1977.

I-10. J.P. Waring and L.E. Hochreiter, PWR FLECHT-SET Phase B1 Evaluation Report, WCAP-8583, August 1975.

Table I-1. Additional BEACH Benchmark Tests Conditions

Test	Flooding Rate in/s	System Pressure psia	Initial Temperature °F	Rod Power kW/ft	Coolant Temperature °F
FLECHT-SEASET TESTS (Reference I-6)					
35807*	0.41	40.0	1628.0	0.27	121.0
35912*	0.42	20.0	1632.0	0.27	93.0
31701	6.1	40.0	1601.0	0.70	127.0
31203	1.51	40.0	1601.0	0.70	126.0
34006	0.59	39.0	1620.0	0.40	124.0
FLECHT FORCED TESTS (References I-9 and I-10)					
8037**	0.40	40.0	1601.0	0.74	128.0
0791**	0.40	15.0	1593.0	0.69	189.0
FLECHT GRAVITY-FEED TESTS (Reference I-11)					
3215B**	Variable	20.0***	1100.0	0.84*****	149.0****
3316B**	Variable	19.0***	1100.0	0.84*****	230.0****

Notes:

* Significant bundle distortion, decay power for group-1 rods reduced (see Section I.2 for details)
** Radial power levels 1.1, 1.0, and 0.95 compared to average power rod (see Section I.3)
*** Containment pressure – see Section I.4 for discrepancy in Test 3316B
**** ECC fluid temperature – see Section I.4 for details
***** The 1.1 power zone was increased – see Section I.4 for details

Table I-2. FLECHT-SEASET Tests (Reference I-6)

FLECHT-SEASET REFLOOD TESTS

Test	Q (kW/ft)	V_{in}(in/s)	Temp Rise (F)	V_{in}/Q (in/s)/(kW/ft)	Temp Rise (F) - BEACH
31701	0.70	6.10	54.00	8.71	43.80
31302	0.69	3.01	79.00	4.36	130.00
31203	0.70	1.51	301.00	2.16	441.50
34006	0.40	0.59	539.00	1.48	799.40
31504	0.70	0.97	593.00	1.39	715.00
31805	0.70	0.81	687.00	1.16	880.00
ftesta_1	0.70	0.72		1.03	970.40
ftesta_4	0.70	0.60		0.86	1165.20
ftesta_3	0.70	0.45		0.64	1567.00
ftesta_2	0.70	0.36		0.51	2048.00
35912	0.27	0.42	586.00	1.56	577.60
35807	0.27	0.41	600.00	1.52	830.40
31701	0.70	6.10	54.00	8.71	
31108	0.70	3.11	96.00	4.44	
31302	0.69	3.01	79.00	4.36	
30921	0.40	1.53	111.00	3.83	
31021	0.40	1.52	91.00	3.80	
30323	0.40	1.52	365.00	3.80	
30223	0.40	1.49	351.00	3.73	
31922	0.40	1.07	166.00	2.68	
33903	0.70	1.58	325.00	2.26	
30518	0.70	1.53	732.00	2.19	
30619	0.70	1.53	871.00	2.19	
30817	0.70	1.52	565.00	2.17	
31203	0.70	1.51	301.00	2.16	
34420	0.74	1.53	189.00	2.07	
34103	0.74	1.50	391.00	2.03	
34610	0.42	0.82	372.00	1.95	
34711	0.42	0.67	474.00	1.60	
34524	1.00	1.57	595.00	1.57	
35912	0.27	0.42	586.00	1.56	
35807	0.27	0.41	600.00	1.52	
34209	0.72	1.07	551.00	1.49	
32013	0.70	1.04	584.00	1.49	
34006	0.40	0.59	539.00	1.48	
31504	0.70	0.97	593.00	1.39	
35304	0.74	1.02	779.00	1.38	
35114	0.74	0.98	550.00	1.32	
34815	0.74	0.98	555.00	1.32	
31805	0.70	0.81	687.00	1.16	

Table I-3. FLECHT Low Flooding Rate Cosine Tests (References I-9 and I-10)

FLECHT LOW FLOODING RATE COSINE TESTS

Test	Q (kW/ft)	$V_{in\ (in/s)}$	PCT T/C Location	T_{max}(^{o} F)	$T_{init\ @}$ PCT Location	DT Rise (F)	V_{in} /Q	DT Rise (F) BEACH
4444	1.22	5.80	4g-6	1963.00	1903.00	60.00	4.75	
6357	0.74	1.50	4g-6	1102.00	1024.00	78.00	2.03	
6458	0.74	1.50	4g-6	1643.00	1625.00	18.00	2.03	
6559	0.74	1.50	4j-6	1456.00	916.00	540.00	2.03	
3113	0.81	1.50	5G-6	1912.00	1557.00	355.00	1.85	
3447	0.89	1.46	5g-6	2006.00	1575.00	431.00	1.64	
4748	0.95	1.51	5g-6	1965.00	1581.00	384.00	1.59	
4831	0.95	1.50	5g-6	1979.00	1575.00	404.00	1.58	
7631	0.95	1.50	5g-6	1916.00	1270.00	646.00	1.58	
8131	0.95	1.50	3h-6	1843.00	1601.00	242.00	1.58	
4930	0.51	0.80	5g-6	1930.00	1586.00	344.00	1.57	
5029	0.73	0.85	5g-6	2075.00	1556.00	519.00	1.16	
7729	0.74	0.79	4h-6	1987.00	1602.00	385.00	1.07	
4641	0.95	1.00	6e-6	2184.00	1495.00	689.00	1.05	
5132	0.95	0.99	5g-6	2138.00	1575.00	563.00	1.04	
2603	0.81	0.81	4F-8	1976.00	830.00	1146.00	1.00	
2414	0.84	0.81	5g-5.6	2263.00	1544.00	719.00	0.96	
2928	0.89	0.80	5g-6.5	2190.00	1586.00	604.00	0.90	
2833	0.89	0.80	5g-6.5	2301.00	1556.00	745.00	0.90	
2326	0.93	0.81	5g-6.5	2213.00	1546.00	667.00	0.87	
6638	0.95	0.82	6e-6	2351.00	1504.00	847.00	0.86	
5239	0.95	0.82	5e-8	2330.00	1230.00	1100.00	0.86	
5543	0.95	0.81	5e-8	2342.00	1352.00	990.00	0.85	
7836	0.74	0.62	5g-6.5	2144.00	1541.00	603.00	0.84	
5342	0.95	0.80	5e-8	2300.00	1211.00	1089.00	0.84	
5636	0.73	0.60	5e-8	2322.00	1326.00	996.00	0.82	
3946	1.22	1.00	5g-6	2272.00	1555.00	717.00	0.82	
1445	1.27	1.00	4g-6	2202.00	1717.00	485.00	0.79	
1545	1.27	1.00	5g-6.5	2169.00	1623.00	546.00	0.79	
7934	0.95	0.62	6g-8	2324.00	1416.00	908.00	0.65	
791	0.69	0.40	5e1	1984.00	974.00	1010.00	0.58	973.20
8037	0.74	0.40	6e-8	2370.00	1369.00	1001.00	0.54	1426.50

FIGURE I-1. PEAK CLAD TEMPERATURE AT ELEVATIONS FLECHT-SEASET TEST 35807.

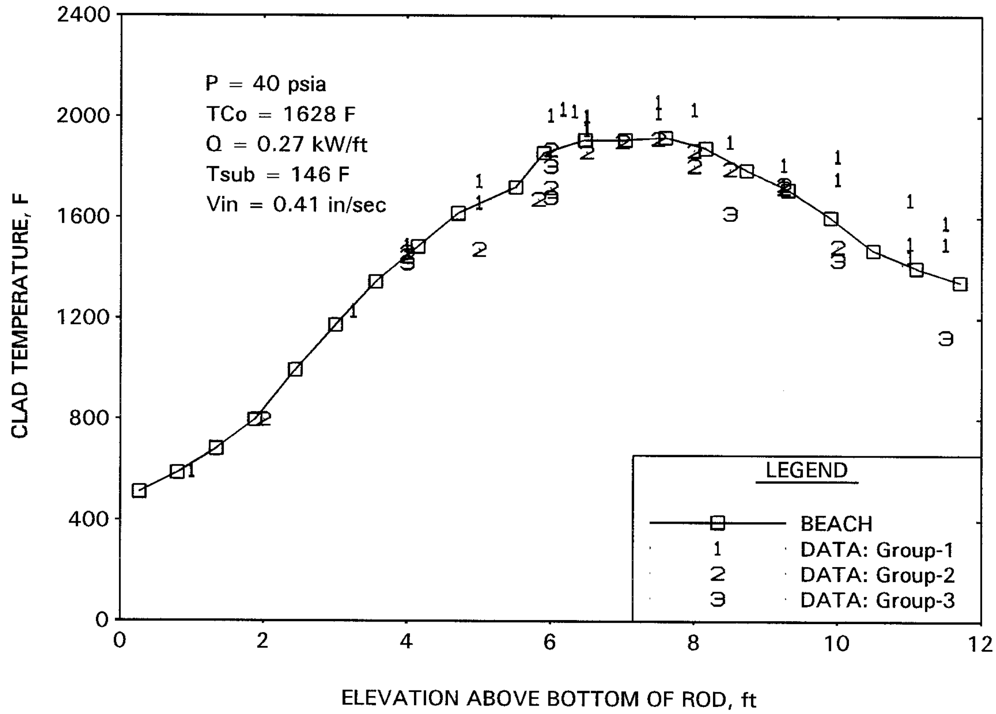

FIGURE I-2. PEAK CLAD TEMPERATURE AT ELEVATIONS FLECHT-SEASET TEST 35912.

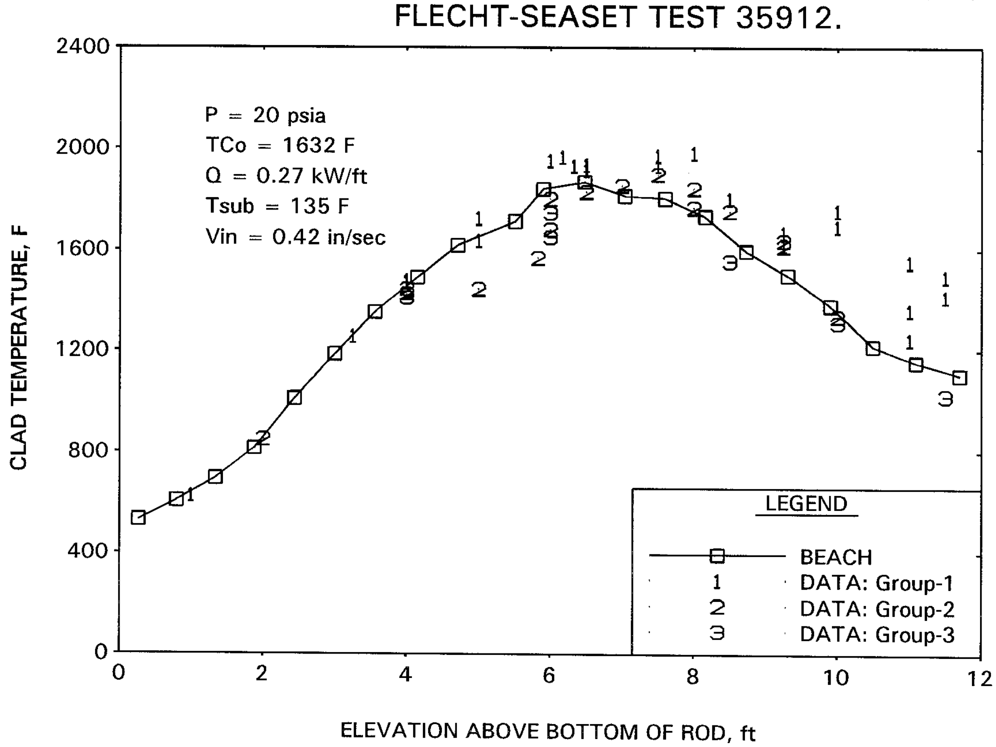

FIGURE I-3. PEAK CLAD TEMPERATURE AT ELEVATIONS FLECHT-SEASET TEST 31701.

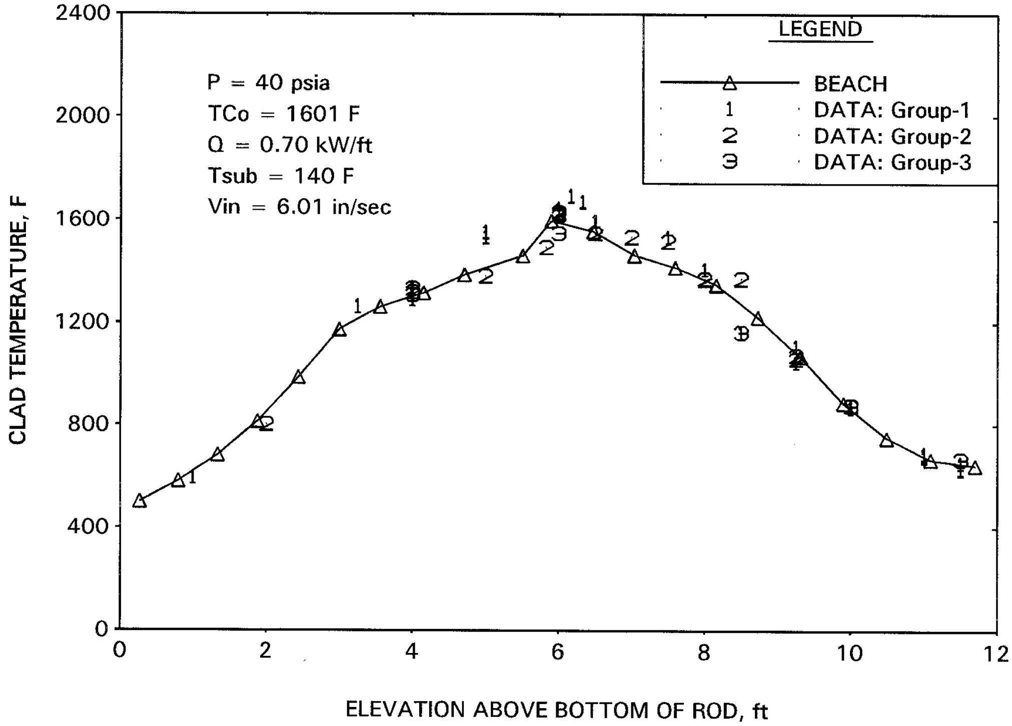

FIGURE I-4. PEAK CLAD TEMPERATURE AT ELEVATIONS FLECHT-SEASET TEST 31203.

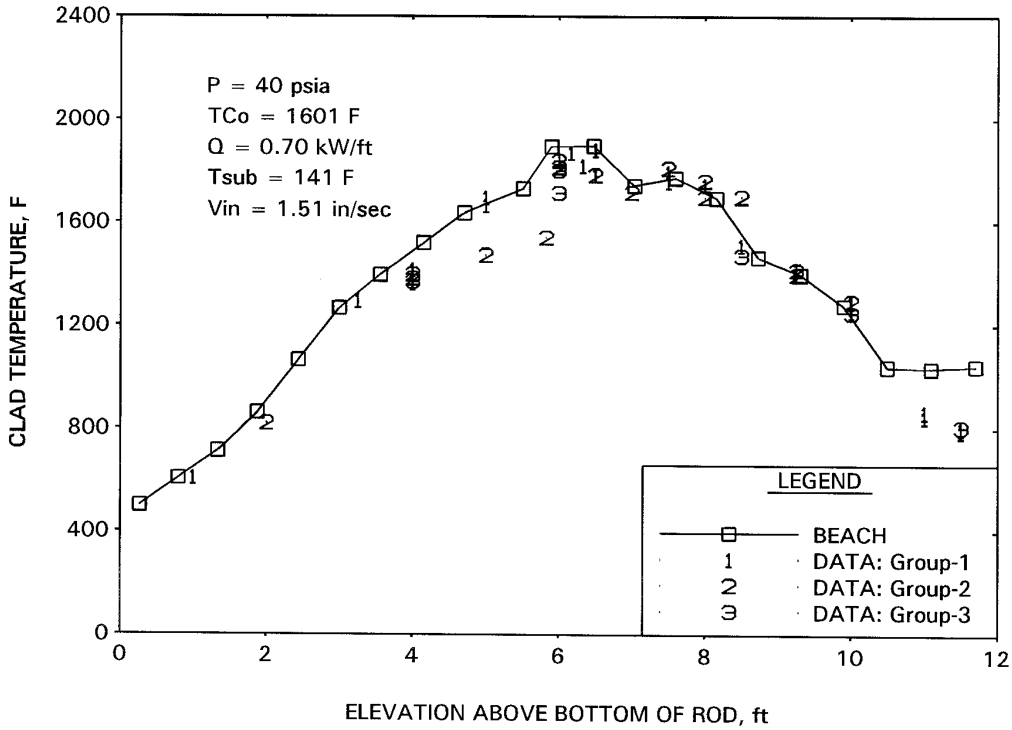

FIGURE I-5. PEAK CLAD TEMPERATURE AT ELEVATIONS FLECHT-SEASET TEST 34006.

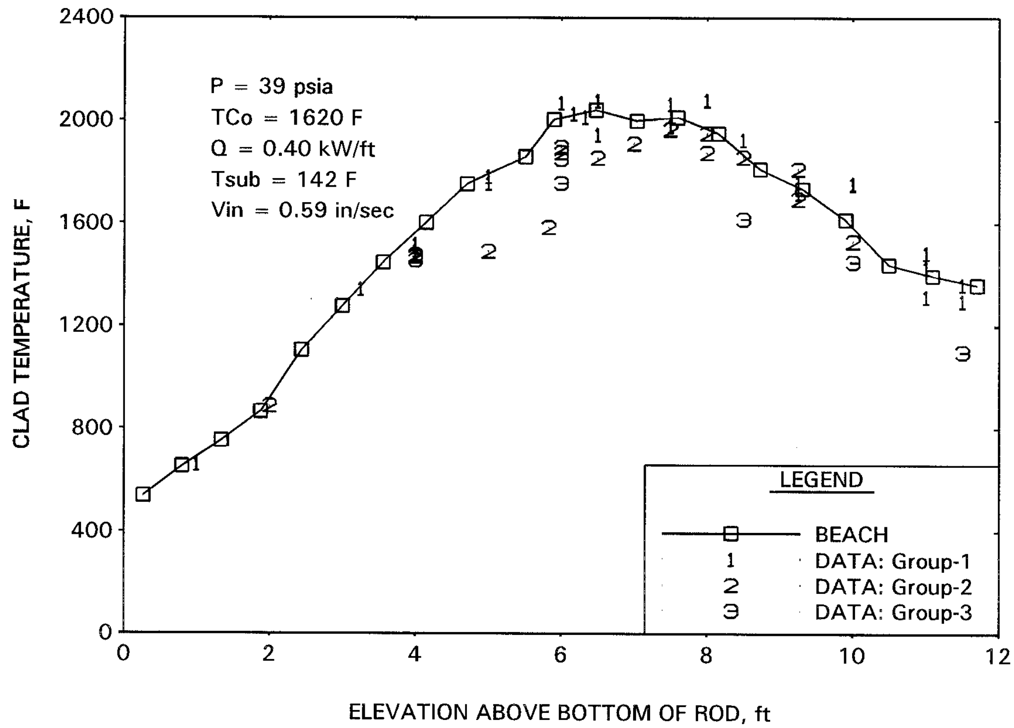

FIGURE I-6. QUENCH FRONT POSITION FLECHT-SEASET TEST 35807.

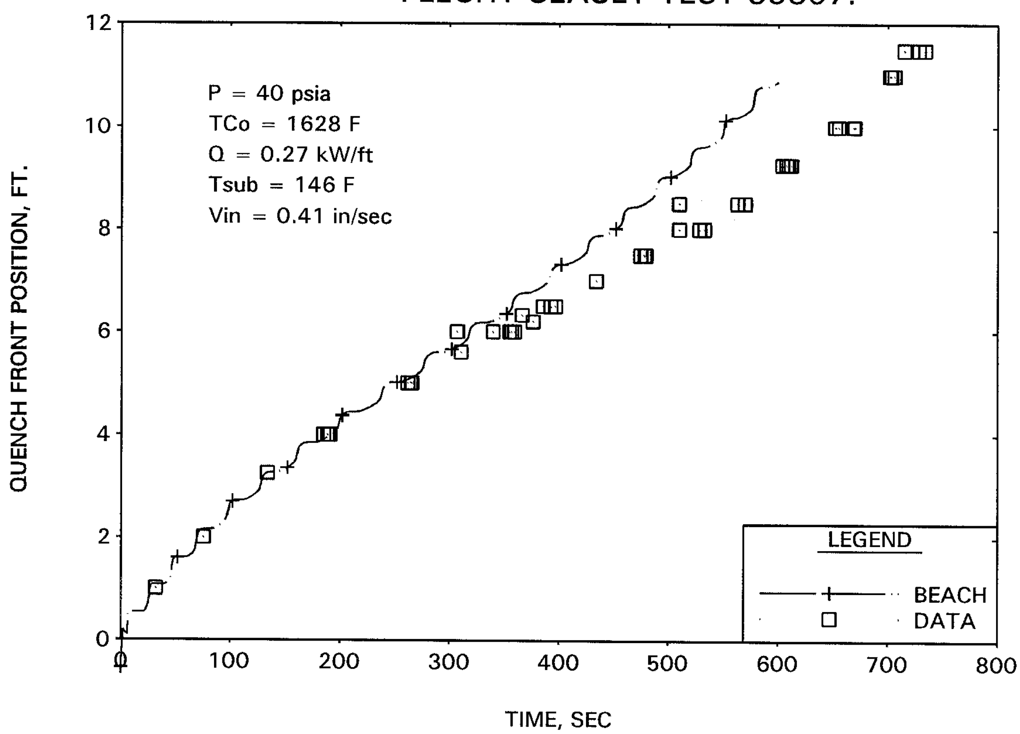

FIGURE I-7. QUENCH FRONT POSITION
FLECHT-SEASET TEST 35912.

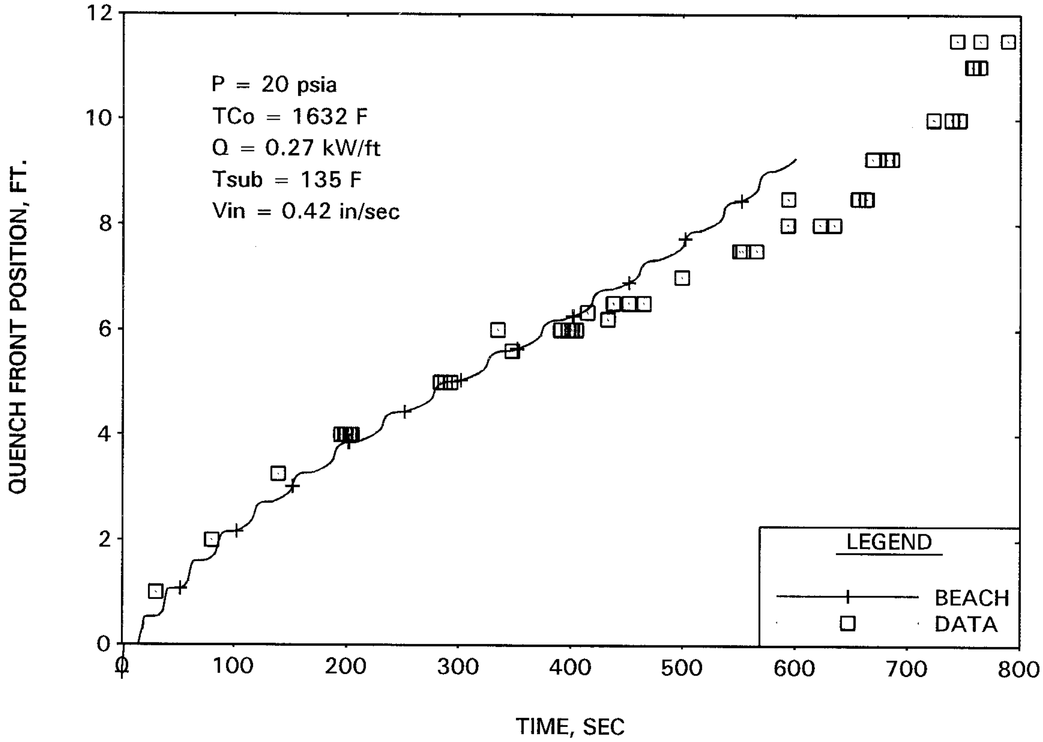

FIGURE I-8. PEAK CLAD TEMPERATURE AT ELEVATIONS FLECHT TEST 8037.

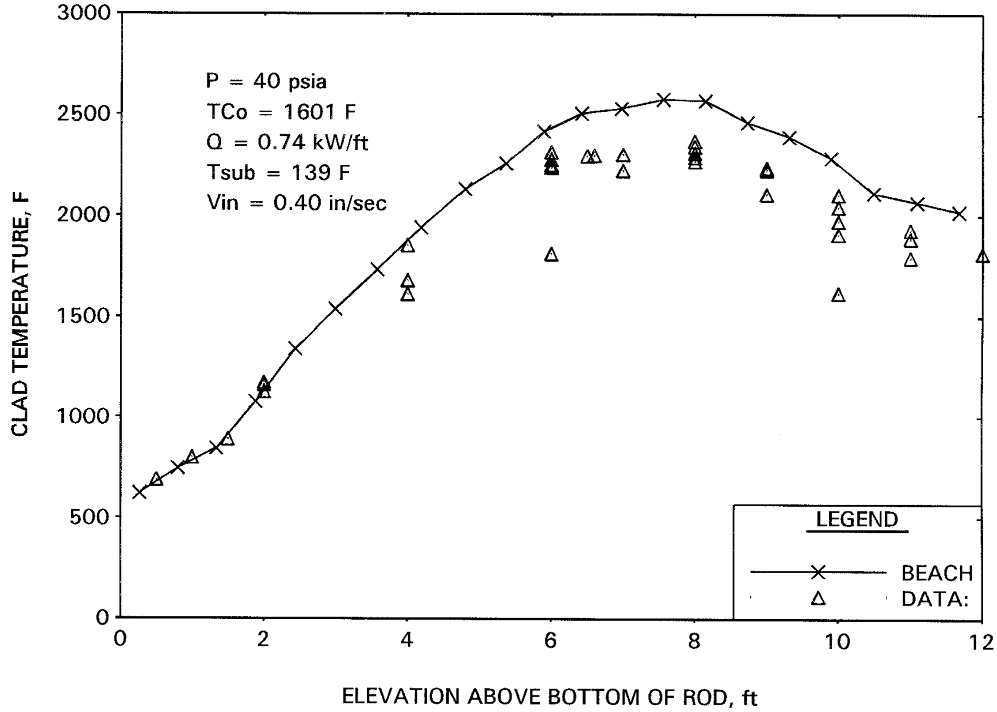

FIGURE I-9. PEAK CLAD TEMPERATURE AT ELEVATIONS FLECHT TEST 0791.

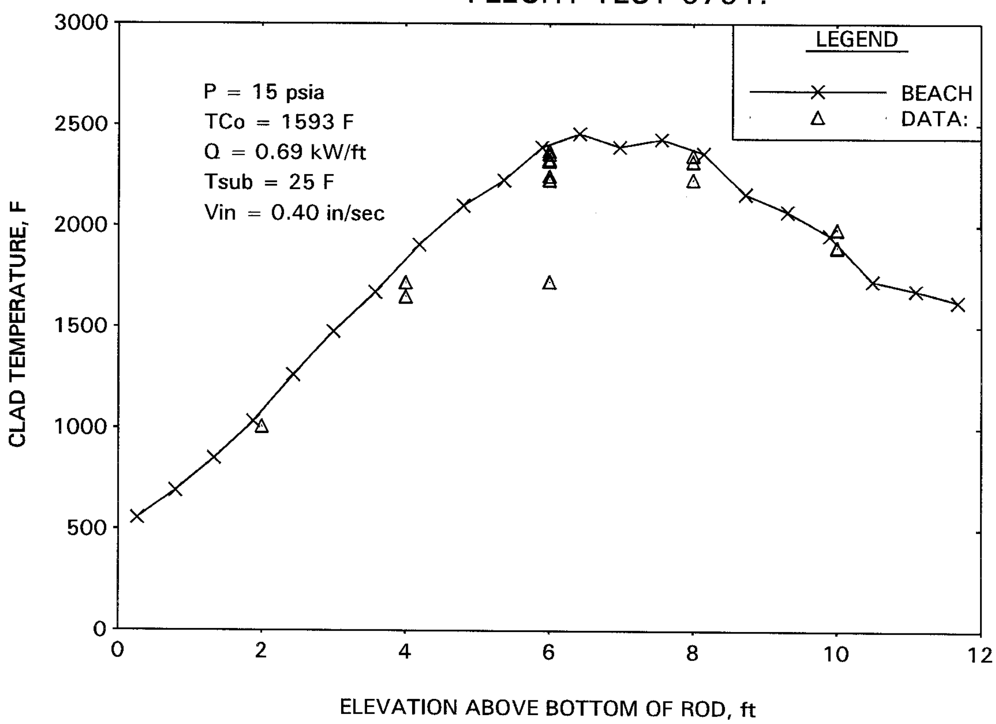

FIGURE I-10. QUENCH FRONT POSITION
FLECHT TEST 8037.

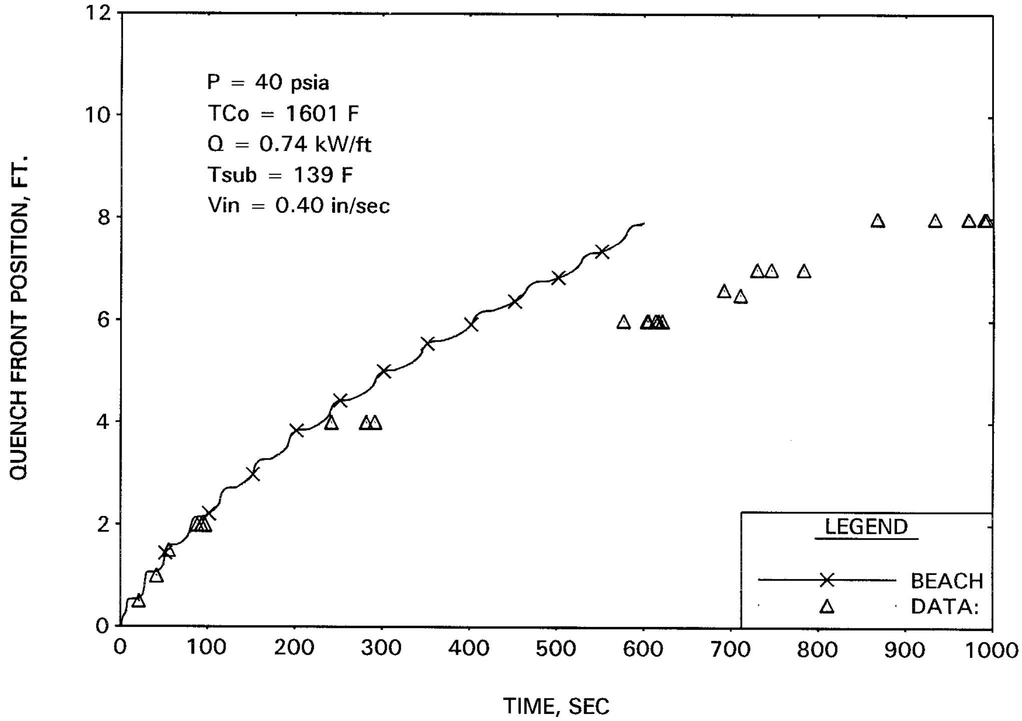

FIGURE I-11. QUENCH FRONT POSITION
FLECHT TEST 0791.

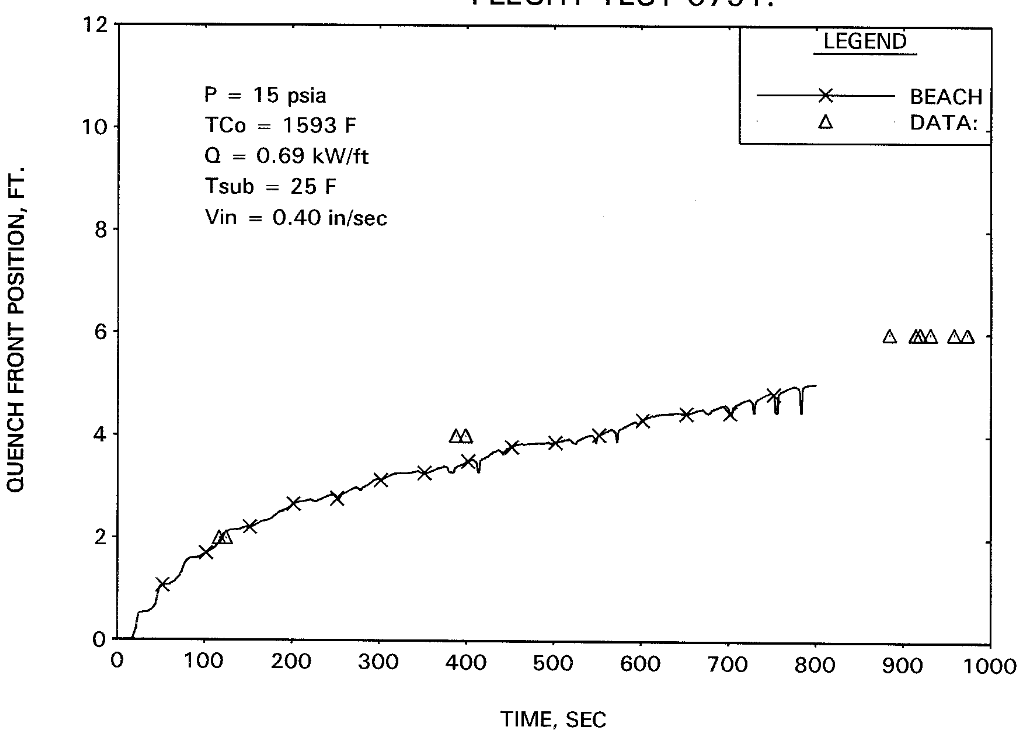

FIGURE I-12. CLAD TEMPERATURE
FLECHT TEST 8037.

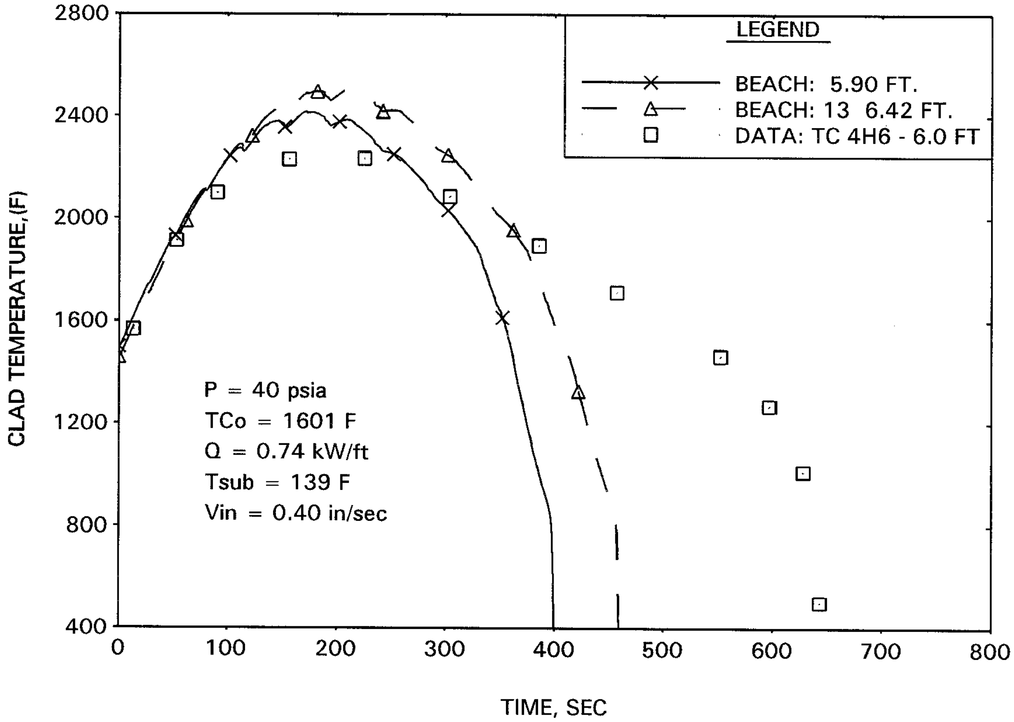

FIGURE I-13. CLAD TEMPERATURE
FLECHT TEST 0791.

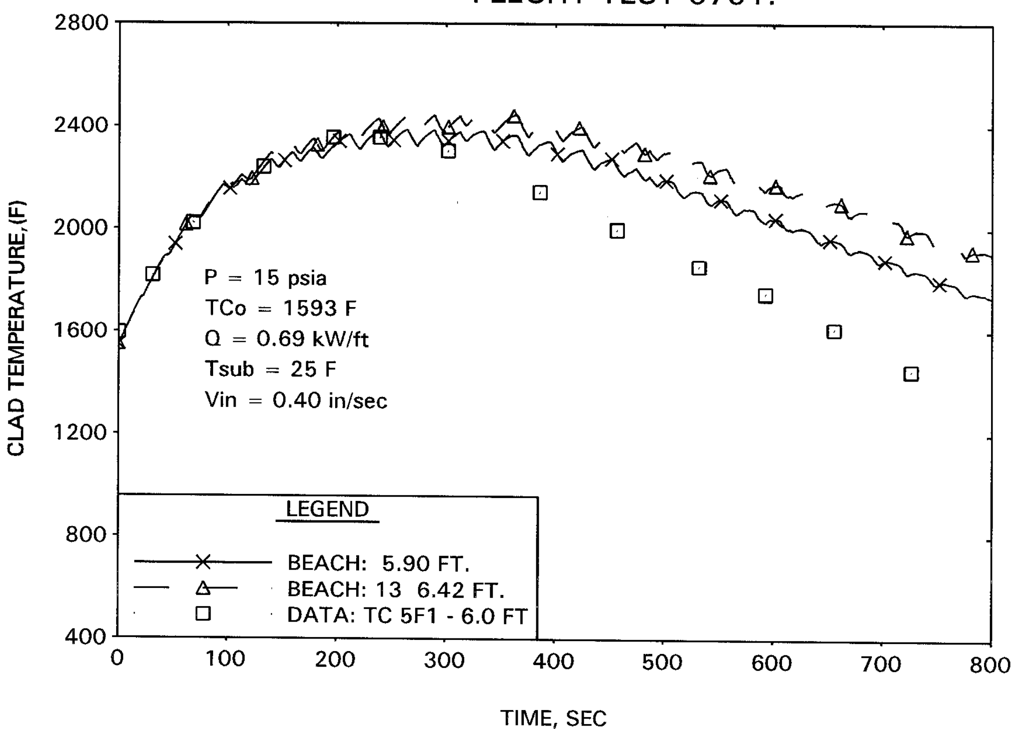

FIGURE I-14. UPPER PLENUM PRESSURE
FLECHT TEST 3215B.

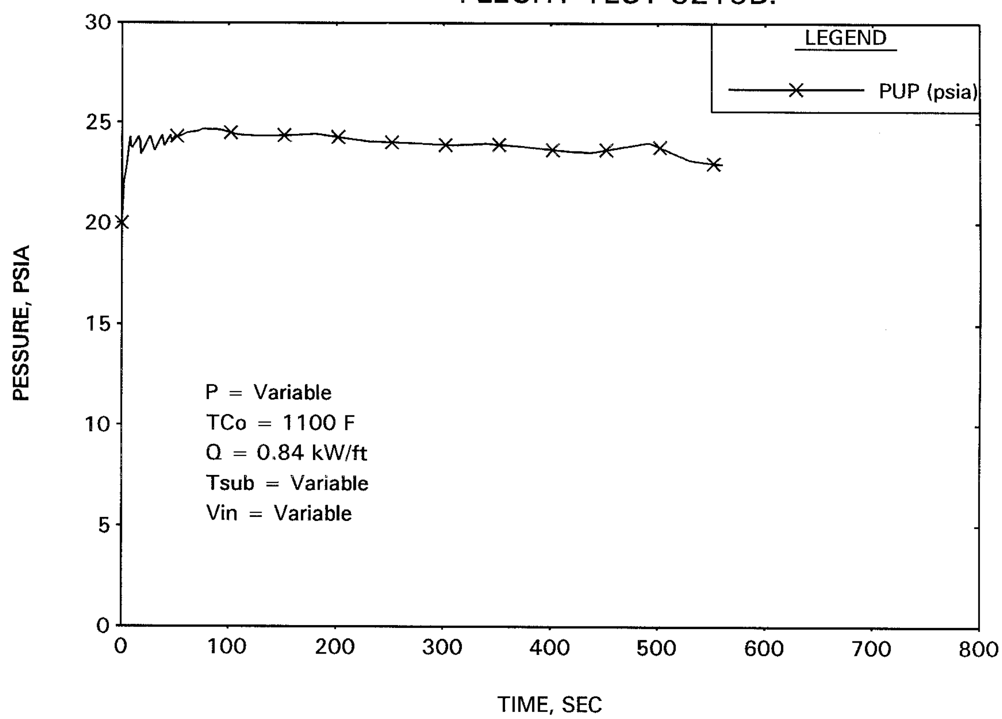

FIGURE I-15. FLOODING RATE
FLECHT TEST 3215B.

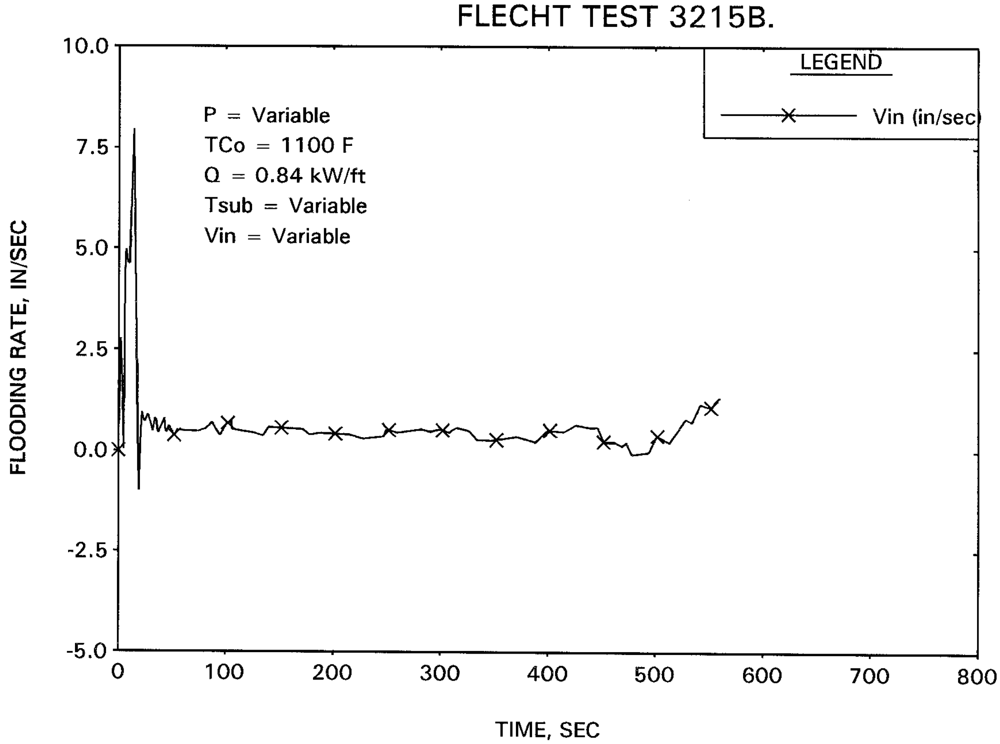

FIGURE I-16. UPPER PLENUM PRESSURE
FLECHT TEST 3316B.

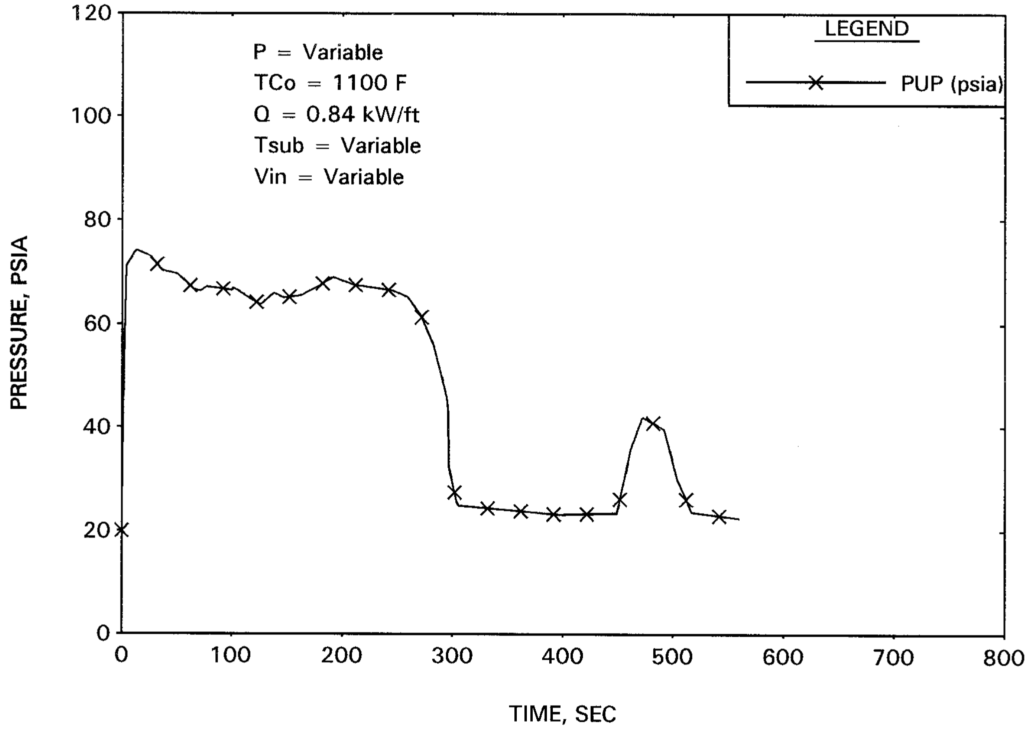

FIGURE I-17. FLOODING RATE
FLECHT TEST 3316B.

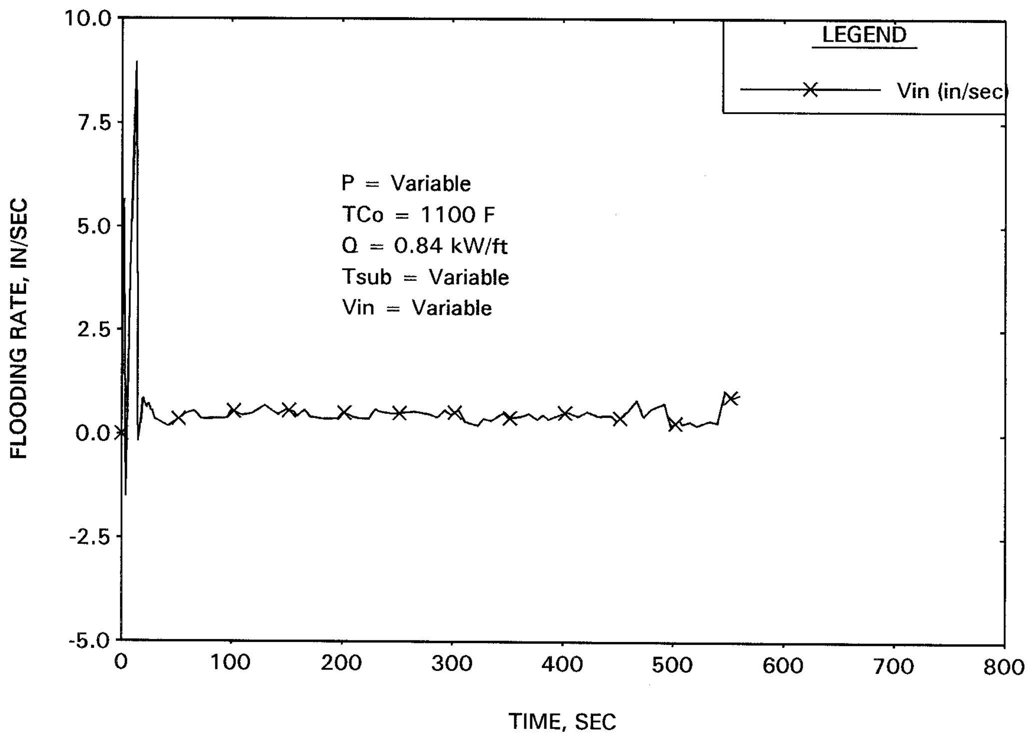

FIGURE I-18. PEAK CLAD TEMPERATURE AT ELEVATIONS FLECHT TEST 3215B.

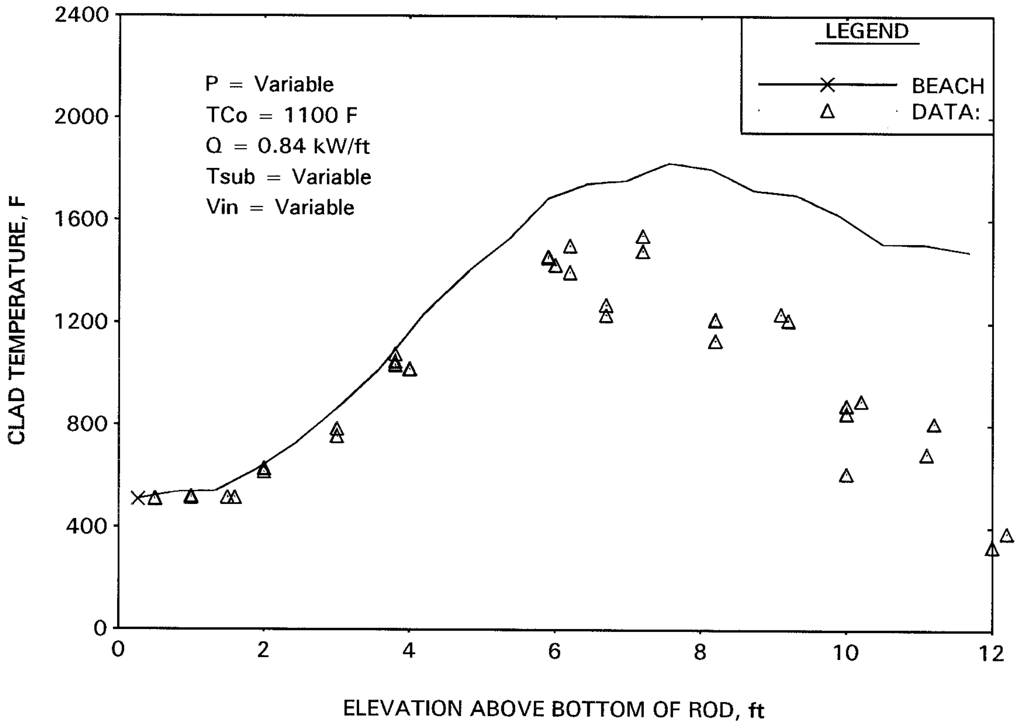

FIGURE I-19. PEAK CLAD TEMPERATURE AT ELEVATIONS FLECHT TEST 3316B.

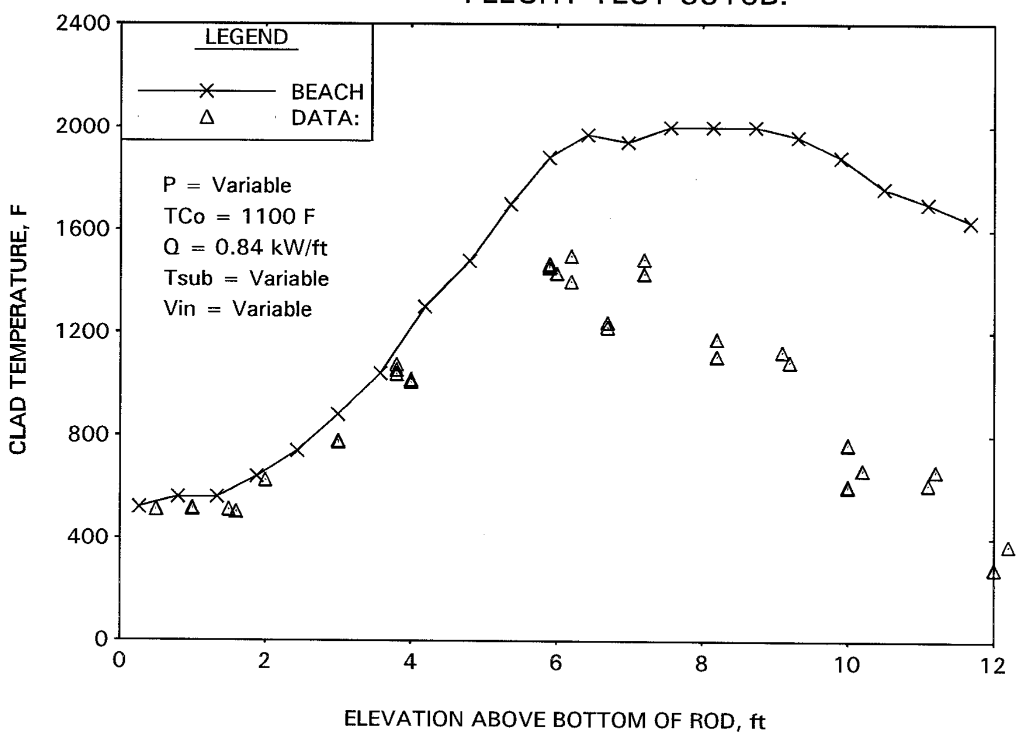

FIGURE I-20. QUENCH FRONT POSITION
FLECHT TEST 3215B.

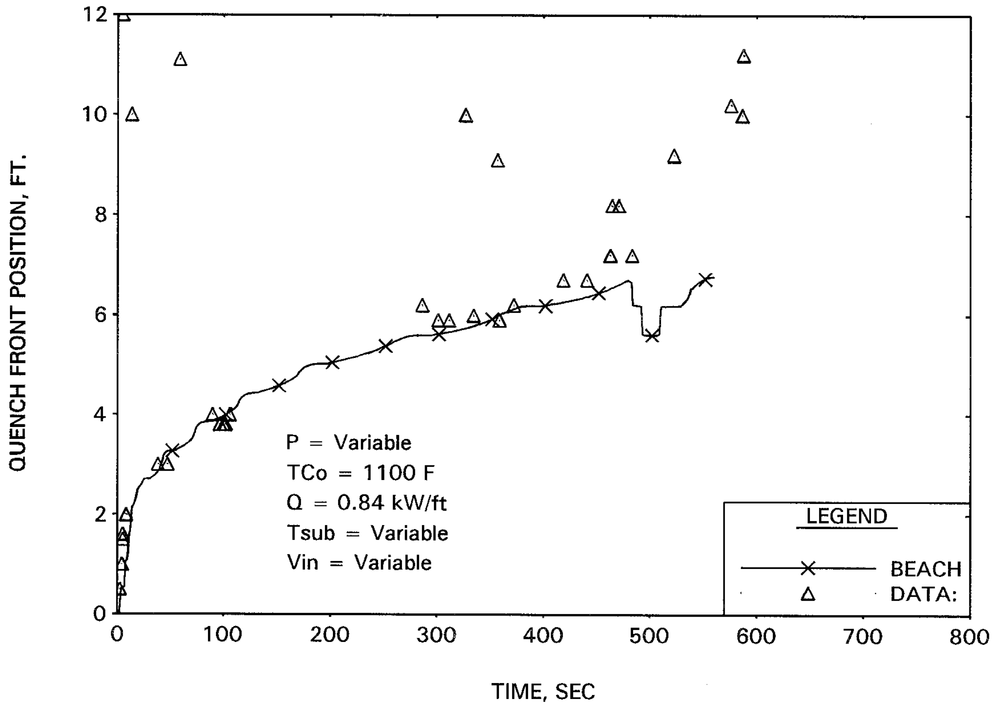

FIGURE I-21. QUENCH FRONT POSITION
FLECHT TEST 3316B.

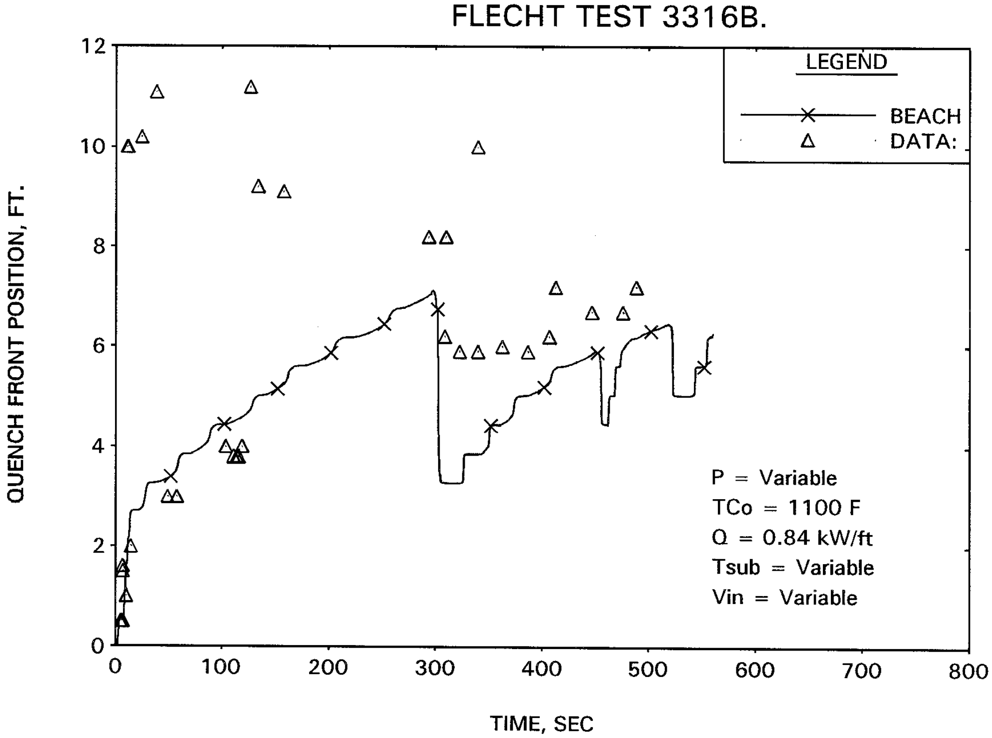

FIGURE I-22. CLAD TEMPERATURE
FLECHT TEST 3215B.

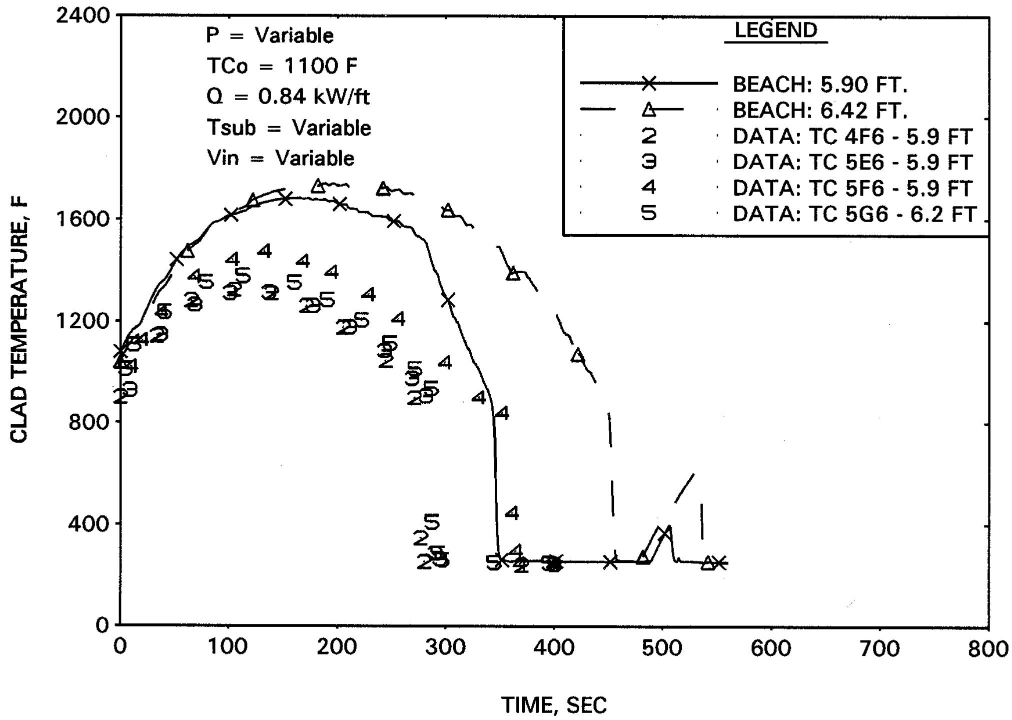

FIGURE I-23. CLAD TEMPERATURE
FLECHT TEST 3316B.

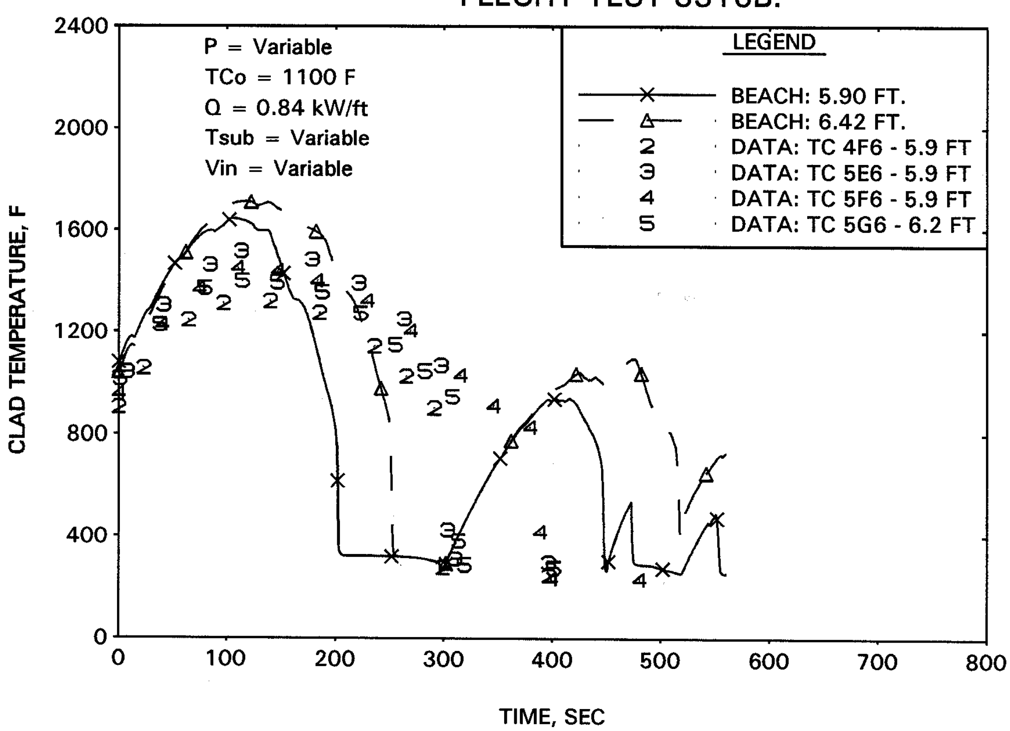

FIGURE 1-24. TEMPERATURE RISE VRS. FLOODING RATE TO ROD PEAK POWER RATIO